JOURNAL OF GEOPHYSICAL RESEARCH: SPACE PHYSICS, VOL. 118, 2970–2974, doi:10.1002/jgra.50182, 2013

The plasma density distribution in the inner region of Saturn's magnetosphere

A. M. Persoon,[1] D. A. Gurnett,[1] J. S. Leisner,[1,2] W. S. Kurth,[1] J. B. Groene,[1] and J. B. Faden[1]

Received 6 November 2012; revised 15 January 2013; accepted 9 February 2013; published 6 June 2013.

[1] Electron density measurements derived from the upper hybrid resonance frequency have been obtained from the Cassini Radio and Plasma Wave Science experiment over a 7 year period from 28 October 2004 through 7 November 2011. Additional density measurements inside the orbit of Enceladus and outside the orbit of Rhea have made it possible to expand a previously published density model to radial distances from 2.6 to 10.0 Saturnian radii (R_S). The distribution of density data is compared to a simple scale height density model for a single-species plasma within 8° of the magnetic equatorial plane. There is a broad peak in the equatorial density distribution between 4 R_S and 5 R_S with the plasma falling off both inward and outward from the peak region. The radial dependence of the equatorial density profile varies as $R^{4.0}$ from 2.6 R_S to 4 R_S and as $R^{-4.8}$ from 5 R_S to 10 R_S. The plasma distribution outside 5 R_S remains consistent with earlier density models but additional density measurements inside 4 R_S provide information on the plasma distribution in this inner region that will be the focus of the F-Ring and proximal orbits near the end of the Cassini mission.

Citation: Persoon, A. M., D. A. Gurnett, J. S. Leisner, W. S. Kurth, J. B. Groene, and J. B. Faden (2013), The plasma density distribution in the inner region of Saturn's magnetosphere, *J. Geophys. Res. Space Physics*, *118*, 2970–2974, doi:10.1002/jgra.50182.

1. Introduction

[2] The plasma in Saturn's magnetosphere has its source in the neutrals, which are emitted from the southern polar region of Enceladus at 3.95 Saturnian radii (R_S). Venting of water molecules produces the narrow Enceladus torus between 3 R_S and 5 R_S [*Johnson et al*., 2006]. Through charge-exchange interactions [*Johnson et al*., 2006; *Jurac et al*., 2002; *Jurac and Richardson*, 2005], electron impact ionization [*Melin et al*., 2009], molecular dissociation [*Jurac and Richardson*, 2005, 2007], ion-neutral collisions [*Jurac and Richardson*, 2007], and neutral-neutral collisions within the torus [*Cassidy and Johnson*, 2010; *Farmer*, 2009], the neutrals expand beyond the narrow Enceladus torus inward to 2 R_S and outward to the orbit of Titan and beyond, forming the expanded neutral OH cloud first observed by the Hubble Space Telescope [*Jurac et al*., 2002; *Shemansky et al*., 1993] and the even broader oxygen cloud observed by the Cassini Ultraviolet Imaging Spectrograph instrument [*Melin et al*., 2009]. Roughly 26–38% of these neutrals are expected to be ionized [*Johnson et al*., 2006; *Jurac and Richardson*, 2007; *Cassidy and Johnson*, 2010]. The ionization of these neutrals by charge exchange, photoionization, and electron-impact ionization is the dominant source of plasma in Saturn's magnetosphere [*Arridge et al*., 2012].

[3] Because the electrons under the influence of a strong ambipolar force [*Persoon et al*., 2009] provide charge neutrality, the distribution of the electrons can be used to map the plasma density in the inner magnetosphere. Electron density measurements derived from the frequency of the upper hybrid emissions and from the Langmuir Probe instrument have been used to develop models of the plasma distribution in Saturn's inner and middle magnetosphere. Early density models derived from Cassini's Radio and Plasma Wave Science (RPWS) electron density measurements focused on mapping the plasma distribution beyond the orbit of Enceladus where densities show a consistent radial dependence from orbit to orbit. A radial distribution model of the equatorial plasma found that the density varied as $R^{-3.7}$ beyond 5 R_S [*Persoon et al*., 2005]. A simple latitudinal scale height model derived from the centrifugal force acting on the plasma was later used to map the distribution of midlatitude plasma beyond 5 R_S for a single-species plasma [*Persoon et al*., 2006]. With the availability of density measurements at higher latitudes in 2007, a diffusive equilibrium model for a two-species plasma was developed. This model yielded separate equatorial ion distributions and an ion scale height for both the water group ions at low latitudes and hydrogen ions at higher latitudes and density contour maps primarily beyond the Enceladus orbit for both ion species and the electrons [*Persoon et al*., 2009]. RPWS Langmuir Probe electron density measurements were also used to create density contour maps out to 20 R_S [*Morooka et al*., 2009].

[1]Department of Physics and Astronomy, University of Iowa, Iowa City, Iowa, 52242, USA.
[2]Blackett Laboratory, Imperial College London, UK.

Corresponding author: A. M. Persoon, Department of Physics and Astronomy, University of Iowa, Iowa City, IA 52242, USA. (ann-persoon@uiowa.edu)

2169-9380/13/10.1002/jgra.50182

[4] Additional density measurements obtained since 2007 have now made it possible to expand the earlier scale height model of *Persoon et al.* [2006] and create a density contour map that extends from 2.6 R_S to 10 R_S. We will show that, in the region of the magnetosphere outside 5 R_S, the radial distribution of the plasma and the plasma scale height derived from the simple scale height density model are consistent with the results of previous studies. Inside 5 R_S, plasma distributions vary from orbit to orbit and few density measurements were available early in the Cassini mission inside 3 R_S to develop a detailed density model. High-inclination orbits in 2008 have provided RPWS electron density measurements down to 2.6 R_S and are used here to model the plasma distribution in the innermost part of the plasma torus where the densities have been shown to be controlled by Saturn's rotation and are highly variable [*Gurnett et al.*, 2007].

2. Simple Exponential-Scale Height Density Model for a Single Species Plasma

[5] Radio and Plasma Wave Science electron densities are used whenever the upper hybrid resonance emission band can be identified from 28 October 2004 through 7 November 2011. his time frame includes high-inclination and mid-inclination orbits as well as equatorial orbits. Figure 1 shows the distribution of RPWS density measurements during this time period. It is our intention to expand the simple exponential scale height model for a single-species plasma [*Persoon et al.*, 2006] to include density measurements in the inner part of the plasma torus. To model a single-species plasma, the density data are restricted to latitudes within 8° of the magnetic equator in a region where water group ions strongly dominate the plasma [*Persoon et al.*, 2009]. Although varying in vertical extent from 2 R_S to 10 R_S, the region within 8° of the magnetic equator is well within ± 3 R_S of the equatorial plane, the near-equatorial region where water group ions have been shown to dominate the plasma [*Thomsen et al.*, 2010, Figure 5]. Restricting our analysis to measurements within 8° of the magnetic equator provides a tighter constraint for the single-species assumption.

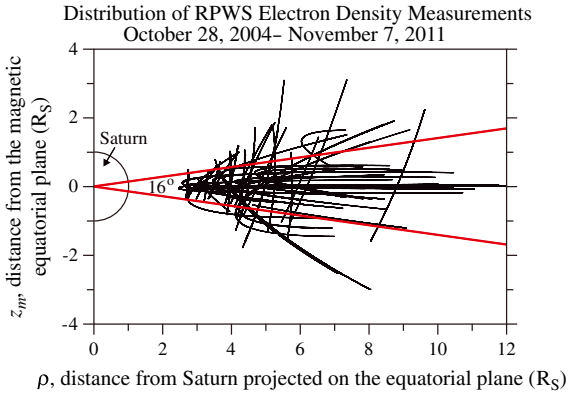

Figure 1. A meridian plane plot showing the distribution of RPWS electron density measurements from 28 October 2004 through 7 November 2011. The red lines indicate the boundaries of the region within $\pm 8°$ of the magnetic equator. Density measurements within this region are used to develop the simple exponential scale height density model for a single-species plasma.

[6] The focus of this paper is on the plasma inside the orbit of Enceladus, but we will also show the plasma distribution out to 10 R_S. The decision to model a single-species plasma is based on the distribution of density measurements inside the orbit of Enceladus, which are largely concentrated within 8° of the magnetic equator. Many of the orbits in the inner part of the plasma torus were high-inclination orbits where the upper hybrid resonance emission band was typically only visible close to the equatorial plane. RPWS density measurements are not available at higher latitudes in this region. A total of 415,000 density values were used to develop this model. Seventy-five percent of these values are in the equatorial region, defined to be $|z_m| \leq 0.1$ R_S, where z_m refers to the perpendicular distance from the magnetic equatorial plane in R_S. The magnetic dipole equator has a small northward displacement from Saturn's rotational equatorial plane of 0.037 R_S [*Dougherty et al.*, 2005].

[7] The simple exponential scale height density model for a plasma dominated by a single ion species is derived by *Persoon et al.* [2006] for plasma densities spanning radial distances of $3.6 \leq L \leq 8.6$ R_S. The model is derived from the centrifugal force acting on the plasma and, for a single-species plasma, results in a simple linear equation for the density

$$\ell n(n_e) = \ell n\left(n_{e,\mathrm{eq}}\right) - \frac{1}{3}\frac{L^2}{H^2}\left(1 - \cos^6\lambda_m\right) \qquad (1)$$

where $\ell n\left(n_{e,\mathrm{eq}}\right)$ refers to the natural log of the equatorial electron density as a function of L, L is the L shell, H is the plasma scale height and λ_m is the magnetic latitude. This study will map the plasma distribution for L shells ranging from $2.6 \leq L \leq 10.0$ R_S.

3. Model for the Plasma Scale Height

[8] In the domain of a single dominant ion species, the analytical form of equation (1) gives a straight line fit for an electron density plot of (ln n_e) as a function of $(1 - \cos^6\lambda_m)$. The slope of that line is equal to $(-1/3)(L^2/H^2)$ [*Persoon et al.*, 2006] and is used to derive the plasma scale height H for each L-shell bin. Because there is considerable scatter in the electron density measurements from orbit-to-orbit, especially inside 5 R_S, the density measurements and the latitude of the spacecraft at the time of the measurements are averaged in nonoverlapping bins of $L \pm 0.1$ with each bin containing one averaged density value and one averaged latitude coordinate for the inbound and the outbound portions of each orbit in the study. The slope of the best line fit through the averaged density values in the plot of (ln n_e) vs $(1 - \cos^6\lambda_m)$ for each L-shell bin is used to derive the plasma scale height for the range of L-shell values. The variation of the scale height with increasing L shell is shown in Figure 2. The best straight line fit through the scale height values for $2.6 \leq L \leq 9.6$ gives a power-law dependence of $H \propto L^{1.5}$, a value consistent with the dependence found by *Persoon et al.* [2009] for the water group ions, the dominant species in the near-equatorial region. It was not possible to determine the scale height for density distributions outside $L = 9.6$ because the density measurements in this region are largely concentrated near the equatorial plane (see Figure 1). The scatter in the plasma scale height values inside 3 R_S and outside 8.5 R_S in Figure 2 is due to the smaller number of density measurements in these

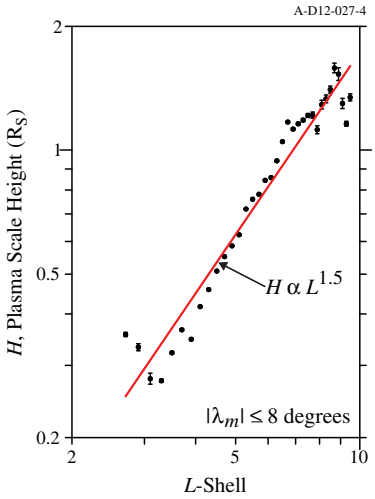

Figure 2. A plot of the plasma scale height as a function of L shell derived from the slope of the best straight line fit for all density measurements plotted as a function of the natural logarithm of the electron density and the parameter $(1 - \cos^6\lambda)$ from equation (1). The best straight line fit through the scale height values for $2.6 \le L \le 9.6$ gives a power law dependence of $L^{1.5}$.

L-shell bins and the large variability in the density measurements from orbit to orbit inside 5 R_S.

4. Model for the Distribution of Equatorial Plasma Inside and Outside $L = 4$

[9] Although the average equatorial density for each L-shell bin can be derived from the y-intercept in the plot of $(\ln n_e)$ vs $(1 - \cos^6\lambda_m)$, we decided to plot all of the equatorial electron densities over the 7 year period and derive a simple radial dependence model to describe the distribution of the equatorial plasma for $2.6 \le L \le 10.0$. The equatorial densities are defined to be density measurements within $|z_m| \le 0.1$ R_S. The radial dependence of Saturn's equatorial plasma is shown in Figure 3a for more than 313,000 electron density measurements. In the region beyond 5 R_S, the density profile shows a consistent radial dependence with small fluctuations on the order of ~30%. The density profile remains identical to previously published equatorial electron density measurements outside 5 R_S [*Gurnett et al.*, 2007; *Persoon et al.*, 2005]. Inside 4 R_S, the electron densities are highly variable from orbit-to-orbit and from inbound-to-outbound portions of the same orbit. This variability has been attributed to longitudinal control of the plasma in this region [*Gurnett et al.*, 2007]. Over the full range of radial distances $2.6 \le L \le 10.0$, the electron density profile in Figure 3a is consistent with the radial dependence of the ion densities derived from the Cassini Plasma Spectrometer (CAPS) [*Thomsen et al.*, 2010, Figure 3c] and the ion densities derived from Langmuir Probe measurements [*Holmberg et al.*, 2012, Figure 4].

[10] To fit a power-law radial dependence model to the equatorial electron density measurements for the regions of the magnetosphere inside and outside the orbit of Enceladus, the density measurements are averaged in non-overlapping L-shell bins of 0.2. The averaged equatorial densities are shown in Figure 3b. There is a broad peak in the equatorial density distribution from 4 R_S to 5 R_S, with the plasma falling off both inside and outside the peak density region. The following hybrid power-law equation is used to fit the equatorial plasma distribution across the full range of L-shell values

$$n^*_{e,\mathrm{eq}} = \frac{n_0}{\frac{1}{2}\left[\left(\frac{R_0}{R}\right)^m + \left(\frac{R}{R_0}\right)^n\right]} \tag{2}$$

where $n^*_{e,\mathrm{eq}}$ refers to the model equatorial electron density, n_0 refers to the density at the peak of the distribution, R_0 refers to the radial distance of the peak, and m and n are the radial dependencies of the plasma distribution inside and outside the density peak, respectively. The solid red line in Figure 3b shows the model fit to the equatorial densities for

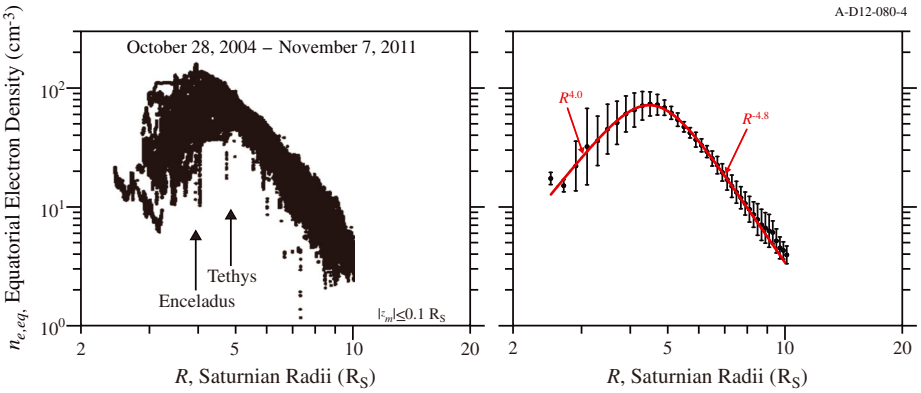

Figure 3. (a) Radial distribution plot of the equatorial densities for $2.6 \le L \le 10.0$ R_S over the 7 year period of this study. Low-density excursions at Enceladus are density measurements taken when Cassini passed through the Enceladus plume. Low-density excursions beyond 6 R_S are density measurements taken when Cassini passed through interchanging flux tubes that are depleted of cold plasma. (b) Plot of the equatorial density measurements averaged in non-overlapping L-shell bins of 0.2. The error bars represent one standard deviation on a log scale on either side of the averaged density values. The solid red line shows the model fit to the equatorial densities using equation (2), which gives a peak density of 72 cm^{-3} at 4.6 R_S and shows the densities increasing with increasing radial distance as $R^{4.0}$ inside the orbit of Enceladus and falling off with increasing radial distance as $R^{-4.8}$ outside 5 R_S.

$2.6 \leq L \leq 10.0$ R_S. The broad density peak in the electron distribution is the result of averaging over many equatorial orbits with large orbit-to-orbit variability in the location of the density peak, which is typically found between 4 R_S and 5 R_S.

[11] The model fit in Figure 3b gives radial dependencies of $m = 4.0$ and $n = 4.8$ and a density peak of 72 cm^{-3} (n_0) at 4.6 R_S (R_0). The density increases with increasing radial distance from Saturn as $R^{4.0}$ inside the orbit of Enceladus and falls off with increasing radial distance as $R^{-4.8}$ outside 5 R_S. In the previous simple scale height density model, the electron density outside 5 R_S was observed to fall off as $R^{-4.1}$ [*Persoon et al.*, 2006]. However, it has also been observed that this exponent changes as equatorial data at larger radial distances are added to a simple scale height density model [*Wilson et al.*, 2008]. *Wilson et al.* [2008] found that the radial distribution of dayside water group ion densities from 5.5 to 11 R_S varied as R^{-5} and the total ion population varied as $R^{-4.8}$, when they applied similar power law fits to density measurements derived from the CAPS experiment.

5. Plasma Density Contour Map

[12] Figure 4 is a plasma density contour plot in the meridian plane (ρ, z_m) for $2.6 \leq L \leq 10.0$. The contour plot assumes azimuthal symmetry about Saturn's rotational axis and mirror symmetry about the magnetic equatorial plane. To produce smoother contours, the equatorial densities and plasma scale heights in Figures 2 and 3b have been smoothed using a 3-point sliding average. A cubic spline fit is then used to interpolate between the averaged density values and plasma scale heights. Plasma scale height values beyond 9.6 R_S are extrapolated from the best line fit in Figure 2. By substituting these values for the equatorial densities and plasma scale heights and incorporating the appropriate magnetic latitude and L values, equations (1) and (2) are used to compute the density at any point (ρ, z_m) in the meridian plane.

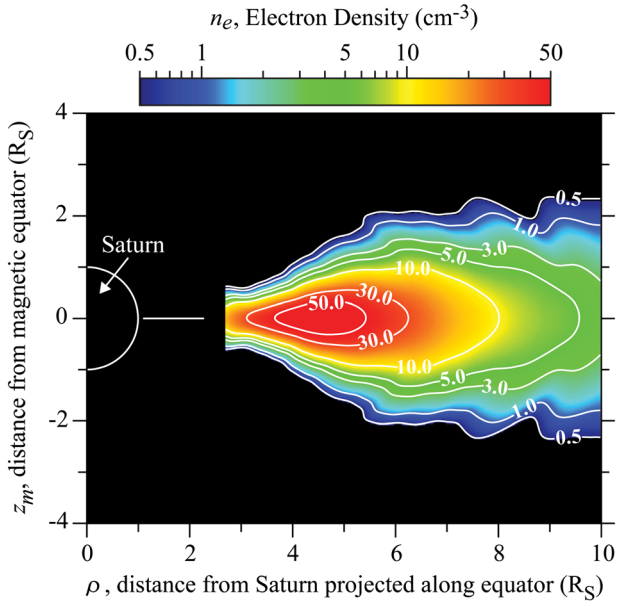

Figure 4. A contour plot of the plasma density in Saturn's inner magnetosphere constructed from a simple exponential scale height model for a single-species plasma, where ρ is the perpendicular distance from Saturn's spin axis and z_m is the distance above/below the magnetic equatorial plane. The contour map shows that the plasma distribution increases with increasing radial distance from Saturn and peaks between 4 R_S and 5 R_S in the magnetic equatorial plane. Beyond 5 R_S, the density decreases with increasing radial distance. At all radial distances, the highest densities are located near the magnetic equatorial plane inside 8 R_S.

[13] The contour map shows that the densest part of the plasma torus ($n_e \geq 10$ cm^{-3}) extends from 2.6 R_S to ~8 R_S with a north-south extension of ± 1 R_S, consistent with the mapping of the electron density contours by *Persoon et al.* [2009, Figure 15] and the mapping of the ion densities over this same radial distance by *Holmberg et al.* [2012, Figure 3]. Beyond 5 R_S, the plasma distribution shown in Figure 4 is qualitatively consistent with earlier plasma density contours derived from models constrained by Voyager measurements [*Richardson and Sittler*, 1990; *Richardson and Jurac*, 2004] and with two Cassini models derived from solutions to field-aligned force balance equations using ion and electron measurements from CAPS and RPWS [*Sittler et al.*, 2008; *Persoon et al.*, 2009].

[14] It is in the region inside 5 R_S that the growing database of Cassini measurements can provide new insight into the distribution of the plasma. Earlier models predicted a plasma distribution near the inner edge of the plasma torus that increases with radial distance from 2 R_S to a density peak at 4 R_S at the orbit of Enceladus [*Richardson and Sittler*, 1990; *Richardson and Jurac*, 2004]. A similar distribution with the plasma diffusing radially outward from Saturn is seen in the density contour maps of *Sittler et al.* [2008], in the ion density profiles [*Thomsen et al.*, 2010; *Holmberg et al.*, 2012] and in the constant density contours of Figure 4. The highest plasma densities (≥ 50 cm^{-3}) peak within a few degrees of the magnetic equatorial plane between ~3.7 R_S and 5.4 R_S. The broad plasma density peak is not centered on Enceladus but is actually centered between the orbits of Enceladus and Tethys. This is in agreement with the broad density peaks in the ion and electron density measurements derived from the CAPS and Langmuir Probe instruments between 4 R_S and 5 R_S [*Sittler et al.*, 2008; *Holmberg et al.*, 2012].

6. Discussion

[15] The simple scale height density model presented here is constrained by electron density measurements within 8° of the magnetic equatorial plane over radial distances of $2.6 \leq L \leq 10.0$ R_S. Specifically, the model describes a plasma dominated by heavy water group ions confined by centrifugal forces to the equatorial plane inside 10 R_S. The dominant source of this plasma is the ionization of water-group neutral particles, which are emitted from the southern polar region of Enceladus at 3.95 R_S and expand both inward and outward to fill Saturn's magnetosphere. The centrifugally-driven ionized plasma diffuses radially outward from the region of Enceladus, varying as $L^{-4.8}$ in the equatorial region beyond 5 R_S.

[16] Inside the orbit of Enceladus, the dominant plasma source is also the water-group neutral particles, which have expanded inward to 2–2.4 R_S where they are deposited on the outer edges of Saturn's main rings [*Jurac and Richardson*,

2007, Figure 2]. The ionization of these neutral particles is the dominant source of torus plasma in the innermost region of the magnetosphere between 2 R_S and 4 R_S. There is also a second plasma source in the tenuous atmosphere of molecular oxygen surrounding the main rings. Ring-ionosphere plasma is created in the space surrounding the ring plane through the photoionization and photodissociation of molecular oxygen [*Bouhram et al*., 2006; *Farrell et al*., 2008] to create a centrifugally driven, outward-flowing plasma, which combines with the torus plasma near the central A ring [*Farrell et al*., 2008]. Inside the Enceladus orbit, this combined plasma varies as L^4 in the equatorial region.

[17] Earlier studies have shown that there is a longitudinal control in the modulation of the plasma density both inside and outside the orbit of Enceladus [*Gurnett et al*., 2007; *Morooka et al*., 2009]. However, density modulations driven by longitudinal variations are not evident in Figures 2 and 3b. The density measurements in each *L*-shell bin can vary up to an order of magnitude over a variety of magnetospheric and temporal conditions and over all longitude values. Averaging these density measurements will mask longitudinal and temporal variations that certainly exist for individual density profiles from single Cassini passes through the inner magnetosphere. The averaged density values in Figure 3b do, however, represent an average between the peaks in the longitudinally-modulated electron density. This is verified by the radial dependence of the plasma outside 5 R_S in Figure 3b where $n_{eq} \propto L^{-4.8}$ falls midway between the L^{-3} and L^{-7} lines, which bound the highest and lowest electron densities modulated by longitude in the study by *Morooka et al*. [2009].

[18] The binning and averaging of all of the equatorial density measurements in Figure 3b shows the plasma expanding radially outward from Saturn to reach a peak between the orbits of Enceladus and Tethys. However, a closer inspection of the individual orbits inside 3.5 R_S (Figure 3a) shows a lot of variability in the plasma distribution, with a few secondary density peaks inside 3 R_S that do not coincide with the Mimas orbit at 3.1 R_S. The plasma distribution inside the orbit of Enceladus does not exhibit the same consistency as the plasma distribution outside 5 R_S and still poses interpretation challenges.

[19] **Acknowledgments.** This research was supported by NASA through contract 1415150 with the Jet Propulsion Laboratory.

References

Arridge, C. S., et al. (2012), Mapping magnetospheric equatorial regions at Saturn from Cassini prime mission observations, *Space Sci. Rev.*, *164*, 1–83, doi:10.1007/s11214-011-9850-4.

Bouhram, M., R. E. Johnson, J.-J. Berthelier, J.-M. Illiano, R. L. Tokar, D. T. Young, and F. J. Crary (2006), A test-particle model of the atmosphere/ionosphere system of Saturn's main rings, *Geophys. Res. Lett.*, *33*, L05106, doi:10.1029/2005GL025011.

Cassidy, T. A., and R. E. Johnson (2010), Collisional spreading of Enceladus' neutral cloud, *Icarus*, *209*, doi:10.1016/j.icarus.2010.04.010.

Dougherty, M. K., et al. (2005), Cassini magnetometer observations during Saturn orbit insertion, *Science*, *307*, 1266–1270.

Farmer, A. J. (2009), Saturn in hot water: Viscous evolution of the Enceladus torus, *Icarus*, *202*, doi:10.10166/j.icarus.2009.02.031.

Farrell, W. M., M. L. Kaiser, D. A. Gurnett, W. S. Kurth, A. M. Persoon, J. E. Wahlund, and P. Canu (2008), Mass unloading along the inner edge of the Enceladus plasma torus, *Geophys. Res. Lett.*, *35*, L02203, doi:10.1029/2007GL032306.

Gurnett, D. A., A. M. Persoon, W. S. Kurth, J. B. Groene, T. F. Averkamp, M. K. Dougherty, and D. J. Southwood (2007), The variable rotation period of the inner region of Saturn's plasma disk, *Science*, *316*, 442–445, doi:10.1126/science.1138562.

Holmberg, M. K. G., J.-E. Wahlund, M. W. Morooka, and A. M. Persoon (2012), Ion densities and velocities in the inner plasma torus of Saturn, *Planet. Space Sci.*, *73*, 151–160, doi:10.1016/j.pss.2012.09.016.

Johnson, R. E., H. T. Smith, O. J. Tucker, M. Liu, M. H. Burger, E. C. Sittler, and R. L. Tokar (2006), The Enceladus and OH tori at Saturn, *Astrophys. J.*, *644*, L137–L139.

Jurac, S., M. A. McGrath, R. E. Johnson, J. D. Richardson, V. M. Vasyliunas, and A. Eviatar (2002), Saturn: Search for a missing water source, *Geophys. Res. Lett.*, *29*, doi:10.1029/2002GL015855.

Jurac, S., and J. D. Richardson (2005), A self-consistent model of plasma and neutrals at Saturn: Neutral cloud morphology, *J. Geophys. Res.*, *110*, A09220, doi:10.1029/2004JA010635.

Jurac, S., and J. D. Richardson (2007), Neutral cloud interaction with Saturn's main rings, *Geophys. Res. Lett.*, *34*, L08102, doi:10.1029/2007GL029567.

Melin, H., D. E. Shemansky, and X. Liu (2009), The distribution of atomic hydrogen and oxygen in the magnetosphere of Saturn, *Planet. Space Sci.*, *57*, 1743–1753, doi:10.1016/j.pss.2009.04.014.

Morooka, M. W., et al. (2009), The electron density of Saturn's magnetosphere, *Ann. Geophys.*, *27*, 2971–2991.

Persoon, A. M., D. A. Gurnett, W. S. Kurth, G. B. Hospodarsky, J. B. Groene, P. Canu, and M. K. Dougherty (2005), Equatorial electron density measurements in Saturn's inner magnetosphere, *Geophys. Res. Lett.*, *32*, L23105, doi:10.1029/2005GL024294.

Persoon, A. M., D. A. Gurnett, W. S. Kurth, and J. B. Groene (2006), A simple scale height model of the electron density in Saturn's plasma disk, *Geophys. Res. Lett.*, *33*, L18106, doi:10.1029/2006GL027090.

Persoon, A. M., et al. (2009), A diffusive equilibrium model for the plasma density in Saturn's magnetosphere, *J. Geophys. Res.*, *114*, A04211, doi:10.1029/2008JA013912.

Richardson, J. D., and S. Jurac (2004), A self-consistent model of plasma and neutrals at Saturn: The ion tori, *Geophys. Res. Lett.*, *31*, L24803, doi:10.1029/2004GL020959.

Richardson, J. D., and E. C. Sittler Jr. (1990), A plasma density model for Saturn based on Voyager observations, *J. Geophys. Res.*, *95*, 12,019–12,031.

Shemansky, D. E., P. Matheson, D. T. Hall, H.-Y. Hu, and T. M. Tripp (1993), Detection of the hydroxyl radical in the Saturn magnetosphere, *Nature*, *363*, 329–331.

Sittler, E. C., Jr., et al. (2008), Ion and neutral sources and sinks within Saturn's inner magnetosphere: Cassini results, *Planet. Space Sci.*, *56*, 3–18, doi:10.1016/j.pss.2007.06.006.

Thomsen, M. F., D. B. Reisenfeld, D. M. Delapp, R. L. Tokar, D. T. Young, F. J. Crary, E. C. Sittler, M. A. McGraw, and J. D. Williams (2010), Survey of ion plasma parameters in Saturn's magnetosphere, *J. Geophys. Res.*, *115*, A10220, doi:10.1029/2010JA015267.

Wilson, R. J., R. L. Tokar, M. G. Henderson, T. W. Hill, M. F. Thomsen, and D. H. Pontius (2008), Cassini plasma spectrometer thermal ion measurements in Saturn's inner magnetosphere, *J. Geophys. Res.*, *113*, A12218, doi:10.1029/2008JA013486.